

Microfluidic device for cell capture and impedance measurement

Ling-Sheng Jang · Min-How Wang

Published online: 17 May 2007
© Springer Science + Business Media, LLC 2007

Abstract This work presents a microfluidic device to capture physically single cells within microstructures inside a channel and to measure the impedance of a single HeLa cell (human cervical epithelioid carcinoma) using impedance spectroscopy. The device includes a glass substrate with electrodes and a PDMS channel with micro pillars. The commercial software CFD-ACE+ is used to study the flow of the microstructures in the channel. According to simulation results, the probability of cell capture by three micro pillars is about 10%. An equivalent circuit model of the device is established and fits closely to the experimental results. The circuit can be modeled electrically as cell impedance in parallel with dielectric capacitance and in series with a pair of electrode resistors. The system is operated at low frequency between 1 and 100 kHz. In this study, experiments show that the HeLa cell is successfully captured by the micro pillars and its impedance is measured by impedance spectroscopy. The magnitude of the HeLa cell impedance declines at all operation voltages with frequency because the HeLa cell is capacitive. Additionally, increasing the operation voltage reduces the magnitude of the HeLa cell because a strong electric field may promote the exchange of ions between the cytoplasm and the isotonic solution. Below an operating voltage of 0.9 V, the system impedance response is characteristic of a parallel circuit at under 30 kHz and of a series circuit at between 30 and 100 kHz. The phase of the HeLa cell impedance is

characteristic of a series circuit when the operation voltage exceeds 0.8 V because the cell impedance becomes significant.

Keywords Single cell analysis · Cell impedance · MEMS

1 Introduction

In the completion the sequencing of the human genome (Consortium 2001; Venter 2001), scientists need to develop new research tools to analyze a vast array of biological information. The growing availability of the genome sequence data is opening up the possibility of developing a comprehensive understanding of complex cellular processes. In traditional approaches, cellular parameters are represented by populations. They are averages and cannot exactly represent individual cells. Additionally, heterogeneity cannot be evaluated in bulk cultures. Multiple parameters must be measured in real time in single living cells to correlate cellular events with genomic information and thus understand complex cellular processes.

For single cell analysis, cell impedance analysis (Gilchrist et al. 2001; Schmukler et al. 1988; Bao et al. 1993) has developed rapidly and has become an effective method of biological measurement. The temperature, electric conductivity and mobility of a cell can influence its impedance characteristics directly or indirectly so the cell impedance characteristic can be used to understand biological characteristic behavior. Measurements on single cells also provide more accurate and in-depth information about electrical properties than do those of pathological tissues. Single-cell impedance also can be applied to study the effect of pharmaceutical compounds (Ye et al. 2003), the effect of viral

L.-S. Jang (✉) · M.-H. Wang
Department of Electrical Engineering and Center for Micro/Nano
Science and Technology, National Cheng Kung University,
1 University Road, Tainan 701, Taiwan
e-mail: lsjang@ee.ncku.edu.tw

and bacterial infections (Niikura et al. 2004; Yang et al. 2003; Verma and Singh 2003; Gau et al. 2001), and environmental parameters (Gilchrist et al. 2005), toxicity (Giaever and Keese 1992) and other factors.

Microsensors are one of the preferred technologies that are adopted to characterize cells according to their electrical properties in the frequency domain for single cell sensing. Recent developments in miniaturized impedance measurement systems enabled the impedance of cells to be measured (Gomez et al. 2001; Gawad et al. 2004; Ayliffe et al. 1999). Impedance studies of cells have demonstrated that the measurement of dielectric properties can reveal the pathological status of the cell. Bio-impedance analysis detects the effects of multiple physiological parameters on gene behavior. In the production of microscale sensors and actuators, micro-electro-mechanical-systems (MEMS) is an enabling technology that is used in semiconductor fabrication (Liao et al. 2005; Jang et al. 2007), and involves the integration of mechanical elements, sensors, actuators, and electronics on a common silicon substrate using micro-fabrication technology. Such microsystems have the potential to lower the cost, increase the accuracy, and reduce the labor involved in performing assays, as compared to macroscale systems. Therefore, the development of MEMS modules for characterizing single cells is essential to measuring multiple parameters in small colonies of living cells in real time.

Stable environments must be maintained for cells of interest to probe cellular functions at the single cell level. Simultaneously, the environment must also be designed to enable effective determination of multiple parameters of cells in real time as functions of environmental changes. In recent years, the general methods used to capture cells have been mechanical trapping, electric trapping and optical tweezers. Mechanical trapping employs MEMS technology and pressure driving to cause fluids to flow through the microchannel. It separates cells of various cell exteriority and sizes (Carlson et al. 1997; Bakajin et al. 1998) or utilizes silicon pillars to catch biological particles (Andersson et al. 2000). Electric trapping uses dielectric characterization of cells to separate them. Xu et al. (2001) demonstrated that the electrodes attracted leukocyte and repelled erythrocyte at frequencies of between 2 and 10 MHz. Fiedler et al. (1998) and Huang et al. (2001) adopted similar approaches to divide various biological particles. Optical tweezers are scientific instruments that use a laser beam to provide an attractive or repulsive force to hold or move dielectric objects. Rusu et al. (2001) and Liang et al. (1994) employed optical tweezers successfully to move and control cells. However, electric trapping may alter the characteristics of a cell because of the high electric field (Weaver and Chizmadzhev 1996) and optical tweezers may damage cells because of the heat generated by the laser

beam. Hence, a method that employs simple three-pillar microstructures as a passive means of capturing single cells physically is developed in this study.

This work presents a microfluidic device for physical capture and measuring impedance by impedance spectroscopy at the single cell level. The device has a PDMS channel and a glass substrate with electrodes. Additionally, an equivalent circuit model is established and fits well with the experimental results of single HeLa cells. Furthermore, the commercial software CFD-ACE+ is used to study the flow around the microstructures in the channel.

2 Materials and methods

2.1 Fabrication of devices

The microfluidic device was composed of a PDMS channel with micro pillars and a glass substrate with electrodes. The PDMS channel was defined using an SU-8 (MicroChem SU-8) mold. The SU-8 was placed on a 4 in. silicon wafer and developed to define structures with a height of 25 μm . The commercially available SYLGARD 184A (pre-polymer)

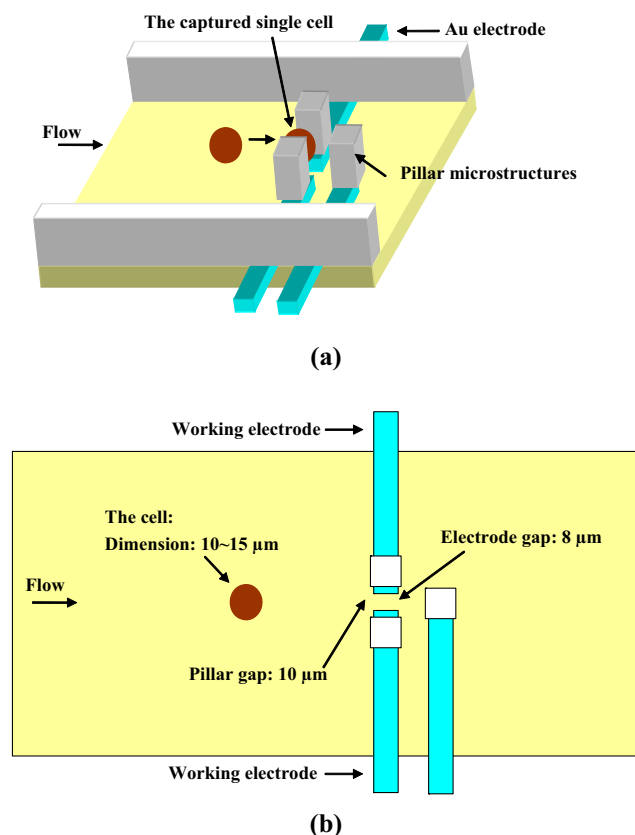


Fig. 1 (a) 3D schematic of the device and complete cell trapping process (b) 2D schematic of the device

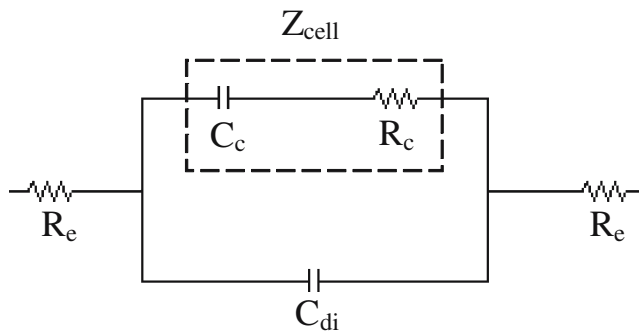


Fig. 2 The equivalent circuit model of the system

and SYLGARD 184B (a curing agent) were mixed with a 10:1 weight ratio and placed on an SU-8 mold. The width and depth of the microchannel were 100 and 25 μm , respectively. The size of the micro pillars was $10 \times 10 \times 25 \mu\text{m}$. The electrodes, including a layer of 15 nm-thick Cr and 65-nm thick Au, were deposited using an E-beam evaporator on glass substrate, patterned by standard photolithographic techniques, and etched using Au and Cr etchant. Finally, the PDMS channel and the glass substrate with electrodes were treated by O_2 plasma (800 W, 12 s) to increase bonding strength. The alignment of the PDMS channel with electrodes was completed in few minutes to prevent loss of O_2 plasma effectiveness. Figure 1 schematically depicts the device and the complete process of cell-trapping.

2.2 Cell culture

In this study, the impedance of HeLa cells (human cervical epithelioid carcinoma) was measured. The HeLa cells were cultured in a humidified incubator at 37°C with 5% CO_2 . The culture medium consisted of 90% minimum essential medium (Eagle) with Eagle’s BSS, 2 mM l-glutamine, 1.5 g/l sodium bicarbonate, 0.1 mM non-essential amino acids, and 1.0 mM sodium pyruvate+10% fetal bovine serum.

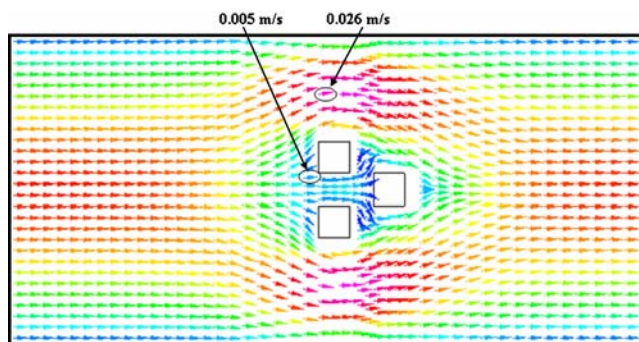


Fig. 3 Velocity field around micro pillars at pressure difference of 100 Pa between and outlet of the channel

3 Theory

An equivalent circuit model, including the cell, dielectric capacitance and electrodes is established. The system can be modeled electrically as cell impedance Z_{cell} in parallel with a dielectric capacitance C_{di} and both in series with a pair of electrodes resistor R_e , as presented in Fig. 2. The model is operated at low frequency between 1 and 100 kHz. Z_{cell} comprises both cell membrane C_c and cytoplasm R_c . C_{di} represents a capacitance that has contributions from all of the materials that are between two electrodes, including the solution. The impedance Z_{cell} is $R_c + 1/j\omega C_c$, where ω is the angular frequency of the electrical single. The overall impedance of the system can be written as

$$Z = 2R_e + \frac{1}{j\omega C_{\text{di}} + \frac{1}{R_c + 1/j\omega C_c}} \tag{1}$$

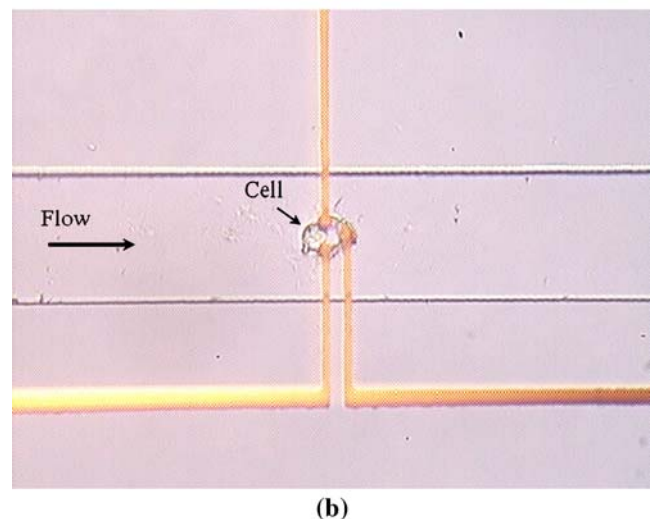
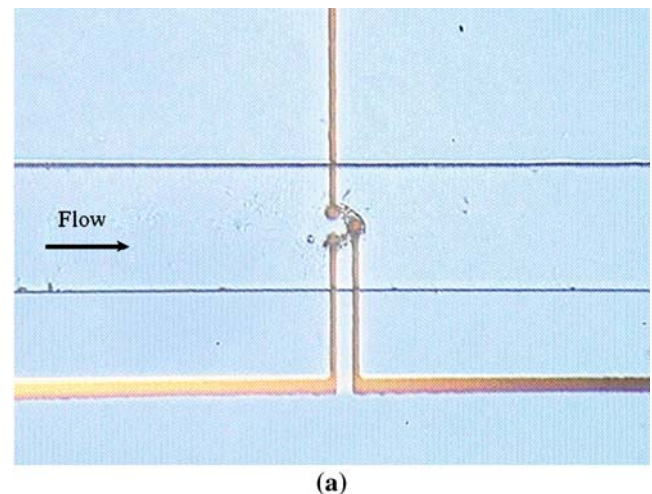


Fig. 4 (a) The cell-trapped structure before injection of cell solution (b) the cell-trapped structure with a single cell of HeLa after injection

Z_R and Z_I are real and imaginary part of Z , respectively, and given by Eqs. 2 and 3.

$$Z_R = 2R_c + \frac{C_c^2 R_c}{(C_c + C_{di})^2 + (\omega C_c C_{di} R_c)^2} \quad (2)$$

$$Z_I = -\frac{1}{\omega} \frac{C_c + C_{di} + \omega^2 C_c^2 C_{di} R_c^2}{(C_c + C_{di})^2 + (\omega C_c C_{di} R_c)^2} \quad (3)$$

4 Simulation

A commercial software package, CFD-ACE+ (CFD Research Corporation), was used to produce a model to study the flow of the channel. The code has unique capabilities for multiphysics, multiscale and coupled simulations of fluid, thermal, chemical, biological, electrical and mechan-

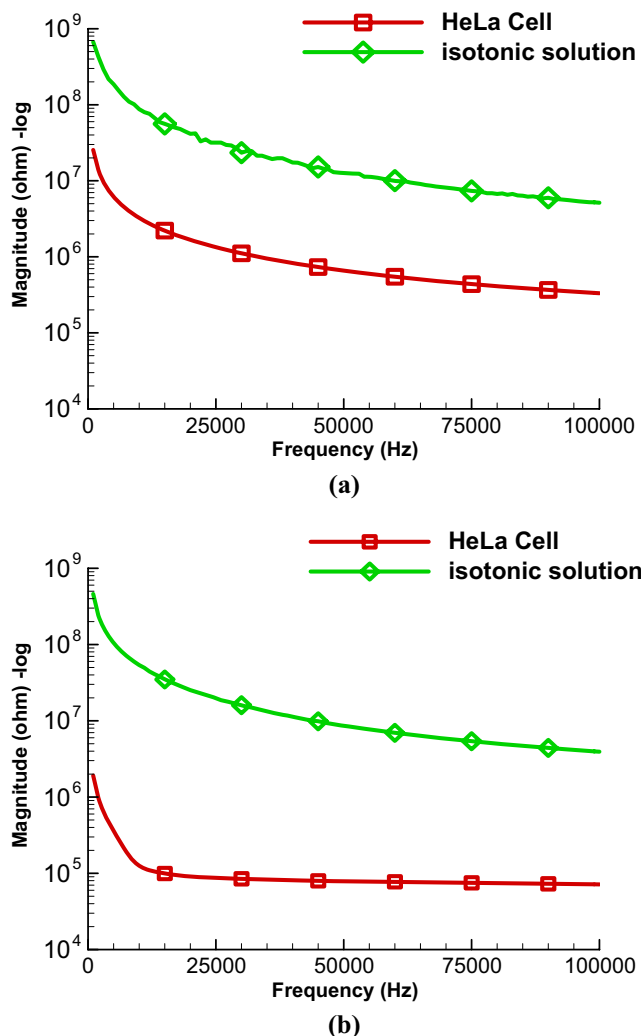


Fig. 5 Impedance magnitude of isotonic solution and the single HeLa cell

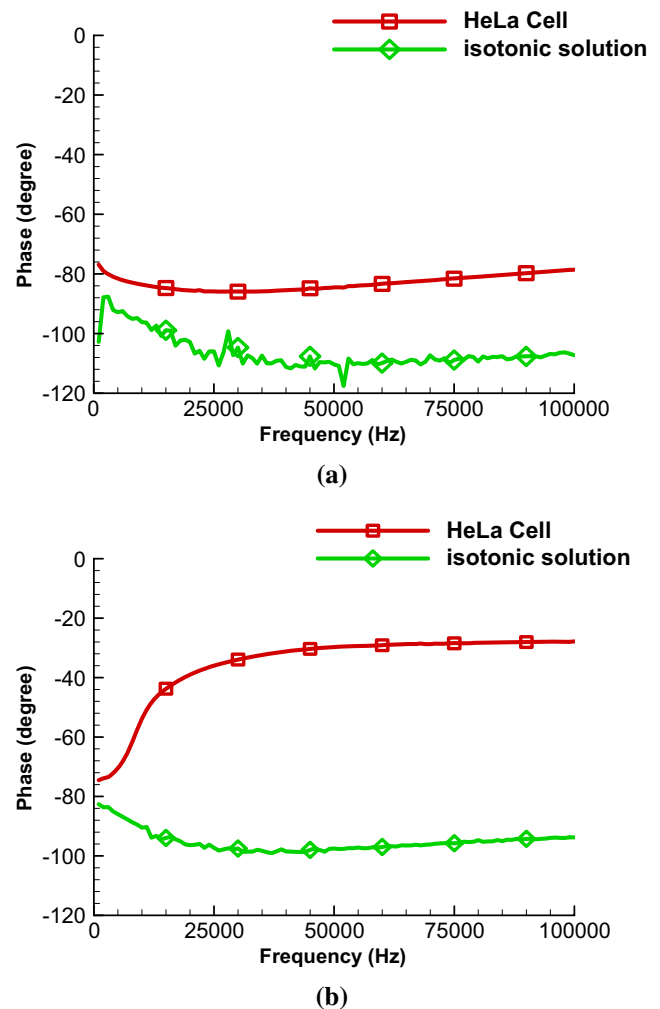


Fig. 6 Impedance phase of isotonic solution and the single HeLa cell at operating voltages of (a) 0.1 V (b) 1.5 V

ical phenomena for real-world applications. The program provided an integrated geometry and grid generation module, a graphical user interface for preparing the model, a computational solver for performing the simulation, and an interactive visualization program. These were used to analyze the simulation results.

Figure 3 presents the velocity field around the micro pillars at a pressure difference of 100 Pa between the inlet and the outlet of the channel. This numerical model was two-dimensional and incorporated a fluid module. The width and length of the model were 200 and 100 μm , respectively, and the size of three micro pillars was $10 \times 10 \mu\text{m}$. The maximum velocity of the fluid near the region of the three micro pillars was about 0.26 m/s. The probability of cell capture was calculated from the percentage of the channel width where the velocity vectors flow into the trap. According to the velocity field, the probability of cell capture by three micro pillars was around 10%.

5 Results and discussion

The micro pillars easily trapped cell debris when the cell solution flowed through the channel, causing the experiment to fail. Accordingly, a protocol with a centrifuge was developed and applied to eliminate the cell debris in the solution. The solution of HeLa cells with a concentration of 2.25×10^5 cells/c.c was injected into the microfluidic channel using an infusion pump (KD Scientific Inc., KDS100) at a flow rate of 5 ml/h. The chips were visually inspected using an optical microscope (Nikon 50i) during the experimental process. Figure 4(a) shows the cell-trapped structures before injection and a single cell of HeLa was trapped successfully among pillars as shown in Fig. 4(b).

When the cell was captured, the infusion pump was switched off to enable the impedance measurement using Precision Impedance Analyzers (Kayne Kerr Inc., 6440B).

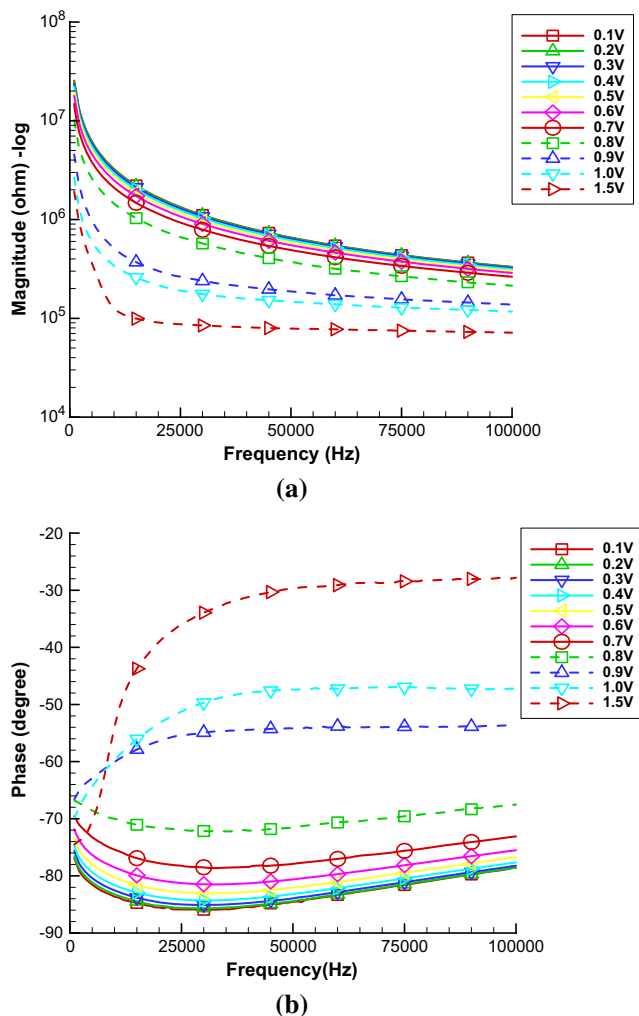


Fig. 7 (a) Impedance magnitude and (b) phase of single HeLa at various operating voltages from 0.1 to 1.5 V

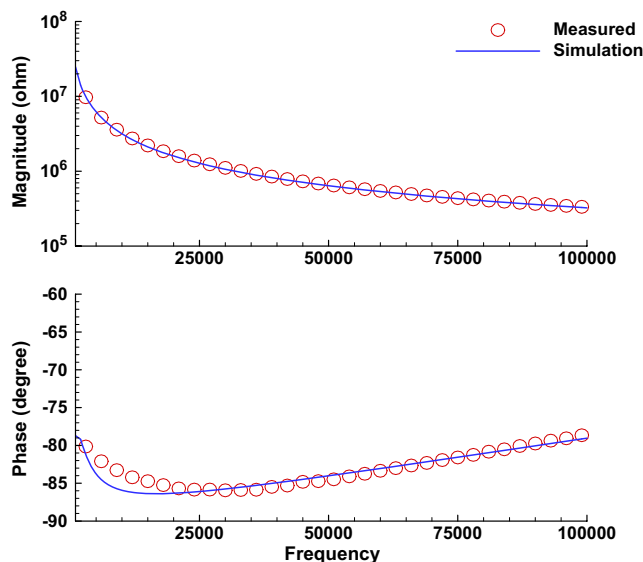


Fig. 8 Plot of simulated (solid line) and measured (circles) system impedance magnitude and phase response at 0.1 V, with parameter $R_c=6 \times 10^7 \Omega$, $C_c=2.5 \times 10^{-12} F$, $R_e=3 \times 10^4 \Omega$ and $C_{di}=5 \times 10^{-12} F$

The 6440B impedance analyzer was self-calibrated, using short and open standard calibration, before the cells were measured. The measurement system was set to the probe station chuck. The Faraday cage was applied to shield electromagnetically the chuck zone. Since the measurement system was capacitive before the samples were injected, the impedance phase angle of the system was -90° at the overall excitation frequency after calibration.

Figures 5 and 6 plot the magnitude and phase of impedance, respectively, as functions of frequency for two different samples (isotonic solution and a single HeLa cell) at operating voltages of 0.1 and 1.5 V. At 0.1 V, the curves of the magnitude and phase were much rougher than those at 1.5 V because the noise was significant when the sample was measured at low voltage. The impedance of isotonic solution at 0.1 V was similar to those at 1.5 V because the electrical resistivity and dielectric of isotonic solution did not vary with the operating voltage. The magnitude of the HeLa cell impedance was smaller than magnitude of isotonic solution about 1~2 orders in both cases, because these cells were more conductive than isotonic solution. At 1.5 V, the cell phase rose from -74.5 to -27.8° between 1 and 100 kHz, in a manner similar to the phase of the series circuit.

Figure 7 plots the impedance of a single HeLa cell at various operating voltages from 0.1 to 1.5 V and frequencies from 1 to 100 kHz. In the frequency range from 1 to 100 kHz, the magnitude of the HeLa cell decreased at all operating voltages: for example, from 2.6×10^7 to $3.3 \times 10^5 \Omega$ at 0.1 V. Increasing the frequency reduced the magnitude of the HeLa cell impedance because the HeLa cell was capacitive. Additionally, increasing the operating voltage decreased the

Table 1 Parameters obtained from fitting circuit model to impedance data

Operation voltage	0.1 V	0.2 V	0.3 V	0.4 V	0.5 V	0.6 V	0.7 V	0.8 V	0.9 V	1.0 V	1.5 V
R_c (Ω)	6.0×10^7	3.9×10^7	3.8×10^7	3.2×10^7	3.0×10^7	2.2×10^7	2.1×10^7	1.9×10^7	1.0×10^7	5.0×10^4	1.0×10^4
C_c (F)	2.5×10^{-12}	4.2×10^{-12}	4.8×10^{-12}	5.0×10^{-12}	6.0×10^{-12}	8.0×10^{-12}	9.0×10^{-12}	1.1×10^{-11}	1.4×10^{-11}	1.8×10^{-11}	7.0×10^{-11}
R_e (Ω)	3.0×10^4	3.0×10^4	3.0×10^4	3.0×10^4	3.0×10^4	3.0×10^4	3.0×10^4	3.0×10^4	3.0×10^4	3.0×10^4	3.0×10^4
C_{di} (F)	5.0×10^{-12}	5.0×10^{-12}	5.0×10^{-12}	5.0×10^{-12}	5.0×10^{-12}	5.0×10^{-12}	5.0×10^{-12}	5.0×10^{-12}	5.0×10^{-12}	5.0×10^{-12}	5.0×10^{-12}

magnitude of the HeLa cell impedance. The impedance of the HeLa cell fell from 1.1×10^6 to $8.5 \times 10^4 \Omega$ between 0.1 and 1.5 V at a frequency of 30 kHz. A strong electric field may open the ionic channels of the cell membrane, increasing ion exchange between the cytoplasm and the isotonic solution (Weaver and Chizmadzhev 1996). Therefore, the electrical resistivity of the cells declines and the dielectric constant of the cells increases. Figure 7(b) plots the phase of the HeLa cell impedance. At an operating voltage of 0.8 V, the phase decreased from -66.9 to -72.2° below 30 kHz because the system impedance response was characteristic of a parallel circuit. In contrast, the phase increased from -72.2 to -67.5° at 0.8 V between 30 and 100 kHz because the system impedance response was characteristic of a series circuit. The phase of the HeLa cell impedance was characteristics of a series circuit when the operating voltage exceeded 0.8 V because Z_{cell} became significant.

The equivalent circuit model of the system including C_c and R_c , C_{di} and R_e shown in Fig. 2 was fitted to the experimental results. The values $R_e = 3 \times 10^4 \Omega$ and $C_{di} = 5 \times 10^{-12}$ F were extracted by curve fitting for the HeLa cell and held fixed when the model was fitted to all other samples. Figure 8 plots simulated (solid line) and measured (circles) system impedance magnitude and phase response at 0.1 V, with parameters $R_c = 6 \times 10^7 \Omega$, $C_c = 2.5 \times 10^{-12}$ F, $R_e = 3 \times 10^4 \Omega$ and $C_{di} = 5 \times 10^{-12}$ F. Table 1 presents the values of C_c and R_c obtained from the fits to all the samples. Since increasing the operating voltage may open ionic channels, R_c declines and C_c increases. Yao et al. (2004) demonstrate that the approximate capacitance of malignant tumor cell membrane is 6.95×10^{-9} F. It is higher than that obtained in this study because they use higher operation voltage (100 V). According to the developed model, it can be seen that the higher operation voltage results in higher cell capacitance.

6 Conclusions

This study presents a microfluidic device that can perform physical capture and measure impedance by impedance

spectroscopy at the single cell level. This microfluidic device comprises a PDMS channel with micro pillars and a glass substrate with electrodes. The experiments reveal that the single HeLa cell is successfully captured by the micro pillars. Its impedance is measured by impedance spectroscopy at frequencies of between 1 and 100 kHz. The commercial software CFD-ACE+ is adopted to study the flow of the microstructures in the channel; the probability of cell capture by three micro pillars is about 10%. Additionally, an equivalent circuit model, incorporating the cell, dielectric capacitance and electrodes, is established. The circuit can be modeled electrically as Z_{cell} in parallel with C_{di} and both in series with a pair of R_e . The equivalent circuit model fits the experimental results closely at various operating voltages. The system parameters can be obtained from the curving fitting of all samples. According to the experimental results for HeLa cell and isotonic solution, the magnitude of the HeLa cell is smaller than magnitude of isotonic solution about 1~2 orders at 0.1 and 0.5 V because this cell is more conductive than isotonic solution. The results of the HeLa cell experiments show that the magnitude of the HeLa cell declines as the frequency increases at all operation voltages because the HeLa cell is capacitive. Furthermore, increasing the operating voltage reduces the magnitude of the HeLa cell impedance because a strong electric field may increase the exchange of ions between cytoplasm and isotonic solution. Below the operating voltage of 0.9 V, the system impedance responds like a parallel circuit below 30 kHz and like a series circuit between 30 and 100 kHz. The phase of the HeLa cell impedance is characteristic of a series circuit when the operating voltage exceeds 0.8 V because Z_{cell} is then significant.

Acknowledgements This work was supported by the National Science Council (NSC 95-2221-E-006-025). Additionally, this work made use of Shared Facilities supported by the Program of Top 100 Universities Advancement, Ministry of Education, Taiwan. The authors would like to thank the Center for Micro/Nano Science and Technology, National Cheng Kung University, Tainan, Taiwan, for equipment access and technical support. The authors also would like to thank National Center for High-Performance Computing, Tainan, Taiwan, for the support of CFD-ACE+.

References

- H. Andersson, W. van der Wijngaart, P. Enoksson, G. Stemme, *Sens. Actuators* **67**, 203–208 (2000)
- H.E. Ayliffe, A.B. Frazier, R.D. Rabbitt, *IEEE J. Microelectromech. Syst.* **8**, 50–57 (1999)
- O. Bakajin, R. Carlons, C. Chou, S. Chan, C. Gabel, J. Knight, T. Cox, R. Austin, in *MicroTAS*, 1998, pp. 193–198
- J.Z. Bao, C.C. David, R.E. Schmukler, *IEEE Trans. Biomed. Eng.* **40** (4), 364–378 (1993)
- R. Carlson, C. Gabel, S. Chan, R. Austin, *Phys. Rev. Lett.* **79**, 2149–2152 (1997)
- I.H.G.S. Consortium, *Nature* **409**, 860–921 (2001)
- S. Fiedler, S. Shirley, T. Schnelle, G. Fuhr, *Anal. Chem.* **70**, 1909–1915 (1998)
- J.-J. Gau, E.H. Lan, B. Dunn, C.-M. Ho, J.C.S. Woo, *Biosens. Bioelectron.* **16**, 745–755 (2001)
- S. Gawad, K. Cheung, U. Seger, A. Bertsch, P. Renaud, *Lab Chip* **4**, 241–251 (2004)
- I. Giaever, C.R. Keese, *Chemtech* **22**, 116–125 (1992)
- K.H. Gilchrist, L. Giovangrandi, G.T.A. Kovacs, in *The 11th International Conference on Solid-State Sensors and Actuators*, Munich, Germany, June 2001, pp. 10–14
- K.H. Gilchrist, L. Giovangrandi, R.H. Whittington, G.T.A. Kovacs, *Biosens. Bioelectron.* **20**, 1397–1406 (2005)
- R. Gomez, R. Bashir, A. Sarikaya, M.R. Ladisch, J. Sturgis, J.P. Robinson, T. Geng, A.K. Bhunia, H.L. Apple, S. Wereley, *Biomed. Microdev.* **3**, 201–209 (2001)
- Y. Huang, K. Ewalt, M. Tirado, R. Haigis, A. Forster, D. Ackley, M. Heller, J. O’Connell, M. Krihak, *Anal. Chem.* **73**, 1549–1559 (2001)
- L.-S. Jang, Y.-J. Li, S.-J. Lin, Y.-C. Hsu, W.-S. Yao, M.-C. Tsai, C.-C. Hou, *Biomed. Microdev.* **9**(2), 185–194 (2007)
- H. Liang, W.H. Wright, C.L. Rieder, E.D. Salmon, G. Profeta, J. Andrews, Y. Liu, G.J. Sonek, M.W. Berns, *Exp. Cell Res.* **213**, 308–312 (1994)
- C.-S. Liao, G.-B. Lee, H.-S. Liu, T.-M. Hsieh, C.-H. Luo, *Nucleic Acids Res.* **33**(18), e156–e162 (2005)
- M. Niikura, A. Maeda, T. Ikegami, M. Saijo, I. Kurane, S. Morikawa, *Arch. Virol.* **149**, 1279–1292 (2004)
- C. Rusu, R. van’t Oever, M. de Boer, H. Jansen, J. Berenschot, J. Bennink, J. Kanger, B. de Grooth, M. Elwenspoek, J. Grever, J. Brugger, A. van den Berg, *J. Microelectromech. Syst.* **10**, 238–247 (2001)
- R. Schmukler, G. Johnson, J.Z. Bao, C.C. Davis, in *IEEE Engineering in Medicine & Biology Society 10th Annual Conference*, vol. 10, no. 2, 1988, pp. 899–901
- J.C.e.a. Venter, *Science* **291**, 1304–1351 (2001)
- N. Verma, M. Singh, *Biosens. Bioelectron.* **18**, 1219–1224 (2003)
- J.C. Weaver, Y.A. Chizmadzhev, *Bioelectrochem. Bioenergetics* **41**, 135–160 (1996)
- J. Xu, L. Wu, M. Huang, W. Yang, J. Cheng, X. Wang, in *MicroTAS*, 2001, pp. 565–566
- L. Yang, C. Ruan, Y. Li, *Biosens. Bioelectron.* **19**, 495–502 (2003)
- C. Yao, C. Sun, Y. Mi, S. Wang, L. Xiong, *Journal of Chongqing University* **27**, 33–35 (2004)
- L. Ye, T.A. Martin, C. Parr, G.M. Harrison, R.E. Mansel, W.G. Jiang, *J. Cell. Physiol.* **196**(2), 362–369 (2003)